Self-trapping and diffusion of hydrogen in Nb and Ta from first principles

Per G. Sundell* and Göran Wahnström†
Department of Applied Physics, Chalmers University of Technology and Göteborg University, SE-412 96 Göteborg, Sweden
(Received 17 March 2004; revised manuscript received 14 July 2004; published 10 December 2004)

Interstitial hydrogen in bcc Nb and Ta is studied theoretically, using first-principles density-functional calculations. The effect of self-trapping is investigated in some detail, and our calculated energies, forces, and displacements for hydrogen at tetrahedral sites are all found to be in good agreement with experiments. The local motion of H and D is treated quantum mechanically by mapping out potential energy surfaces and solving a Schrödinger equation for the ground state and vibrationally excited states. Diffusion between sites is discussed in both the classical and the quantum regimes. At low temperatures, the small-polaron theory of phonon assisted tunneling is applied, and we find excellent agreement with experiments for both the calculated coincidence energy and bare tunneling matrix elements. At higher temperatures our results indicate that hydrogen migration should best be described in terms of overbarrier motion, rather than tunneling from excited states.

DOI: 10.1103/PhysRevB.70.224301 PACS number(s): 66.35.+a, 71.15.−m, 66.30.Jt

I. INTRODUCTION

The properties of hydrogen-metal systems have attracted a lot of attention.[1] From an applied point of view, they are relevant for understanding the mechanisms at work in important technical areas such as hydrogen storage, fuel cells, and hydrogen embrittlement. From a more fundamental point of view, hydrogen in metals might serve as a model problem for theoretical investigations of more complicated systems. In particular, the small mass of the hydrogen isotopes allows for the study of quantum nucleus phenomena in condensed matter. For example, zero-point motion effects, discrete vibrational energy levels, and the possibility of tunneling have all been observed for H in metals.[2]

The properties of H–group-V bcc transition metals (V, Nb, Ta) have been studied extensively, both experimentally and theoretically. In the dilute α phase, dissolved hydrogen has been found to preferably occupy tetrahedral sites in the lattice. Hydrogen diffuses rapidly in these materials and retains a high mobility even down to very low temperatures where quantum effects should dominate. Indeed, experimentally one has found a change of the activation energy around 250 K for hydrogen diffusion in Nb and Ta, using both the Gorsky effect[3] and nuclear magnetic resonance (NMR) measurements.[4] This has been explained in terms of incoherent tunneling between hydrogen ground states localized on neighboring sites.[5,6]

Hydrogen in bcc hosts has previously been investigated theoretically by several different approaches. The use of various model potentials has provided valuable insight regarding the properties of self-trapped hydrogen states, their coupling to the lattice, and their rate of migration.[7–11] The application of empirical potentials is, however, severely limited by the requirement of accurate estimates of some relevant quantities describing the H-metal interaction. Methods based on *ab initio* simulations[12,13] are unbiased in this respect, but normally require a classical description of the nuclei in the system of consideration. Thus it is difficult to access properties related to the light interstitials being quantum mechanically delocalized. Such examples are activation energies and transfer integrals for phonon-assisted tunneling.

In a previous Letter[14] we demonstrated the validity of the Flynn-Stoneham model[5] for H diffusion in Nb and Ta in the temperature range $100\ \mathrm{K} < T < 200\ \mathrm{K}$, solely based on first-principles density-functional theory (DFT) calculations. This was done using a straightforward scheme to represent a delocalized hydrogen nucleus in the tunneling configuration. In this paper a more detailed investigation is made regarding the hydrogen-lattice coupling. We have calculated total energies and the induced forces and resulting displacements of surrounding metal atoms for hydrogen occupying different interstitial sites at varying concentrations. The discussion about hydrogen diffusion is also extended to include the high-temperature regime. This allows for a direct comparison between lattice-assisted quantum tunneling and classical overbarrier migration.

II. METHODOLOGY

A. Hydrogen–host-lattice coupling

Our starting point is to consider a system consisting of a hydrogen interstitial and a metal host. If the electronic degrees of freedom are eliminated with the usual Born-Oppenheimer approximation, the interaction potential is determined by solving an electronic structure problem. This can be done accurately and efficiently using DFT. We also assume the light hydrogen atom to be adiabatically decoupled from the motion of the much heavier metal atoms, and the latter are treated as classical particles.

To lower the total energy of the system, a hydrogen located at some stable site in the lattice will distort the positions of the surrounding metal atoms. The gain is the so-called *self-trapping* energy. As a consequence, the translational symmetry of the crystal is destroyed so that if a hydrogen is moved from its initial site i to a neighboring site f, without allowing the lattice to readjust, the energy will be higher. At low temperatures, this prohibits tunneling between the sites. Thermal fluctuations of atomic positions might, however, create a lattice configuration where levels of i and f become equivalent and tunneling can take place. The minimum energy required to establish this configuration is the

so-called *coincidence* energy. This quantity gives the activation energy for phonon-assisted tunneling diffusion at low temperatures.[5,6] It is also an important measure of the coupling of a moving impurity to the host lattice vibrations.[1] At higher temperatures, classical overbarrier motion is instead expected to be the dominating diffusion mechanism. The corresponding *classical migration* barrier is calculated as the energy required to move the hydrogen, by an adiabatic deformation of the lattice, over the saddle point separating sites i and f.

In principle, these distortions of the lattice should be calculated by optimizing atomic positions in the presence of a hydrogen density corresponding to the localized vibrational ground states. However, since only a small isotope effect in the volume expansion of hydrogen loaded crystals have been observed,[15] this should be a minor effect. Also, in Ref. 16 it was found, using a pair-potential description for the H—Pd system, that inclusion of the finite extension of the hydrogen wave function only changed the energy of the self-trapped state by a few percent, compared with treating the interstitial as a pointlike classical particle.

When relaxing the lattice to the self-trapped and classical saddle-point configurations, the hydrogen is therefore treated as a pointlike particle. For a tunneling interstitial in the coincidence configuration, one obviously has to relax this assumption. In the spirit of the other calculations we treat the delocalized hydrogen as a superposition of two point particles with equal weight and placed at neighboring sites i and f, respectively. The average force on a surrounding metal atom from these localized parts is then given by a weighted sum of Hellmann-Feynman forces that is evaluated using symmetry considerations.

B. Localized hydrogen vibrations

Vibrational states of the interstitial are determined by exploiting the fact that the hydrogen mass is much smaller than the mass of the host metal atoms. If a hydrogen nucleus can be assumed to respond adiabatically to any motion of the host lattice, the impurity will be moving in a potential field generated by the the instantaneous positions of the surrounding metal atoms. We have considered two different sets of equilibrium ionic positions, which correspond to hydrogen in the self-trapped and coincidence states. For these energy relaxed lattice configurations we map out three-dimensional potential energy surfaces (PES's). The hydrogen motion is treated quantum mechanically, so that vibrational states are calculated by solving a Schrödinger equation where the wave functions are required to vanish on the boundaries of a sufficiently large "box" enclosing the stable interstitial sites. For the self-trapped state, the resulting wave functions can be characterized by the irreducible representations of the point symmetry group of the occupied site. From the calculated energy levels, vibrational excitation energies are extracted. For the coincidence configuration, tunneling matrix elements are estimated from the splitting of odd and even states in the symmetric potential.

C. Computational details

Our calculations are based on DFT within the plane-wave pseudopotential method. To solve the Kohn-Sham equations we use the Vienna *ab initio* simulation package[17,18] (VASP). The electron-ion interaction is described by the projector augmented-wave method.[19] For the exchange-correlation part we use a generalized gradient approximation (GGA) due to Perdew and Wang.[20] The Brillouin zone sampling was performed using the Monkhurst-Pack method.[21] For the calculation of the fractional occupancies, a Methfessel-Paxton smearing technique[22] was employed with $N=1$ and $\sigma=0.2$ eV. All calculations were performed non-spin-polarized with a plane-wave cutoff of 250 eV. Using this setup an equilibrium lattice constant of 3.32 Å was found for both metals in their bcc structure, in good agreement with experiments. Atomic hydrogen was introduced in primitive supercells containing N^3 metal atoms and conventional cubic supercells containing $2\times N^3$ metal atoms for $N=1$, 2, and 3 to estimate the effect of finite hydrogen concentrations in the materials.[33]

The PES's for hydrogen vibrational motion are mapped out on regular grids by repeating the calculations for several different positions of the hydrogen atom within the supercell. Interpolation with piecewise cubic Hermite polynomials is used to map the PES on to a finer grid where the vibrational Schrödinger equation is discretized with finite differences. The resulting eigenvalue problem is solved using the Lanczos algorithm with selective reorthogonalization.[34]

III. RESULTS AND DISCUSSION

A. H-Nb and H-Ta lattice energies, forces, and displacements

We first consider the problem of site occupation. In Table I the calculated energies for hydrogen occupying different

TABLE I. Calculated energies (in eV/atom) for a hydrogen impurity at different interstitial sites in bcc Nb and Ta in the low-concentration limit. The energies are given relative to the pure host metal and an isolated hydrogen dimer as $E=E_{\text{H-metal}}-E_{\text{metal}}-\frac{1}{2}E_{\text{H}_2}$.

	Niobium		Tantalum	
Location	Fixed	Relaxed	Fixed	Relaxed
T site	−0.201	−0.389	−0.228	−0.413
M point	+0.110	−0.240	+0.083	−0.227
S point	+0.103	−0.241	+0.078	−0.233
O site	+0.465	−0.096	+0.480	−0.077

TABLE II. Calculated forces and lattice distortion for hydrogen occupying *T* and *O* sites in Nb and Ta. The forces exerted by a hydrogen impurity on nearest-neighbor and second-nearest-neighbor metal atoms in an unrelaxed lattice are denoted by F_1 and F_2, respectively. From these, the derived quantities of the force-dipole tensor are evaluated. Also given is the displacement u_1 of the nearest-neighbor metal atoms upon self-trapping.

	Niobium		Tantalum	
	T site	*O* site	*T* site	*O* site
F_1 (eV/Å)	1.2	3.2	1.2	3.3
F_2 (eV/Å)	0.2	0.3	0.2	0.4
$2A+B$ (eV)	11.0	13.2	11.7	14.4
$\lvert A-B\rvert$ (eV)	0.3	9.3	0.1	9.2
u_1 (Å)	0.08	0.19	0.07	0.18

interstitial sites in a fixed and a relaxed host lattice at low hydrogen concentrations (1/54) are given. In particular, we have investigated the tetrahedral (*T*) and octahedral (*O*) sites, as well as the mid (*M*) and saddle (*S*) points separating two neighboring tetrahedral sites in Nb and Ta. For both metals, *T* sites are found to be the most stable. The energy differences of around 0.7 eV between *T* sites and *O* sites and around 0.3 eV between *T* sites and *M* points in the fixed lattice agree well with the results of Elsässer *et al.*[12] Further, our calculated energies for hydrogen occupying relaxed *T* sites are consistent with with the experimental heat of solution −0.35 eV/atom for Nb and −0.39 eV/atom for Ta.[23]

We next consider the interaction of hydrogen atoms with the host lattice in some detail. The directions of the forces exerted by a hydrogen impurity on surrounding metal atoms are given by the local symmetry of the occupied interstitial site. In Table II the magnitude of the calculated forces exerted by a hydrogen at *T* and *O* sites on the nearest- and second-nearest-neighbor metal atoms are given. The magnitude *F* of the induced force field decays quite rapidly with distance *d* from the nearest defect in the host crystal. An exponential fit $F(d) \propto \exp[-d/d_0]$ gives for both H-Nb and H-Ta a mean extension $d_0 = 0.2a$ for hydrogen at the *T* site and $d_0 = 0.1a$ for hydrogen at an *O* site. Direct measurements of these forces are difficult, but the components of the force-dipole tensor *P*, defined as

$$P_{ij} = \sum_m F_i^m R_j^m, \tag{1}$$

are accessible from experiments. Here $\mathbf{F}^m$ is the Kanzaki force[24] on metal atom *m* located at a position $\mathbf{R}^m$ from the defect. For hydrogen occupying tetrahedral or octahedral sites in a bcc lattice, this rank-2 tensor is diagonal with $\mathrm{Tr}P \equiv 2A+B$ proportional to the isotropic volume expansion of a hydrogen loaded crystal. Similarly, the quantity $|A-B|$ can be taken as a measure of the anisotropy of the induced force field. As pointed out previously,[13] evaluating the force-dipole tensor from first principles presents a number of difficulties. When approximating $\mathbf{F}^m$ by the Hellmann-Feynman forces calculated within a plane-wave pseudopotential approach, care must be taken to use sufficiently large supercells so that the force field close to any given interstitial is similar to that of an isolated hydrogen. Alternatively, symmetrization

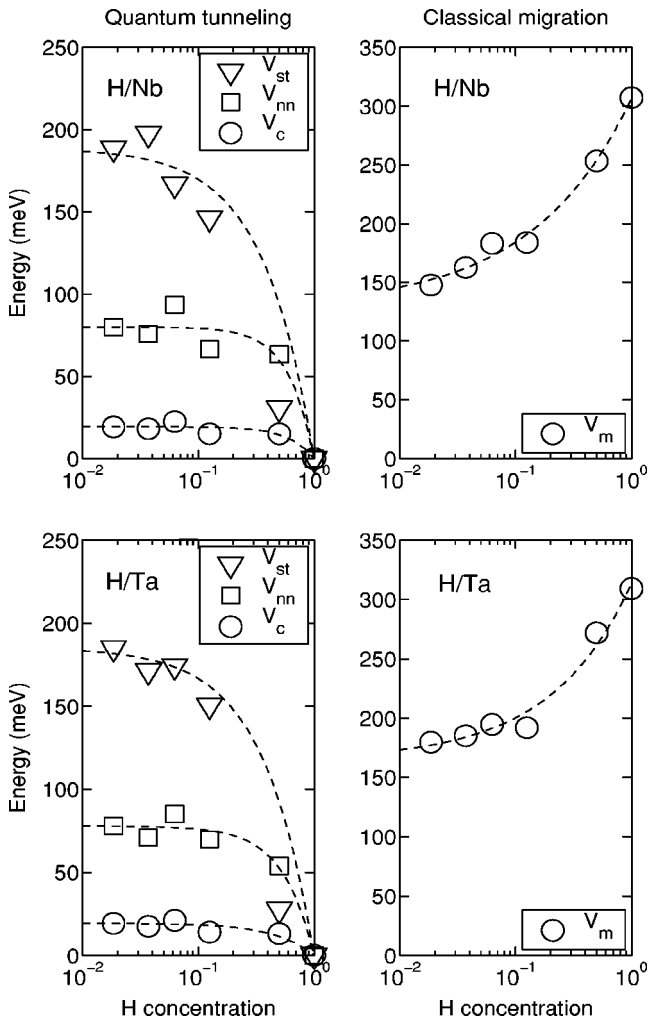

FIG. 1. Characteristic energies for quantum and classical diffusion of hydrogen between neighboring *T* sites in Nb and Ta, calculated for different sizes of supercells. Left panels show the convergence of quantities describing lattice-assisted quantum tunneling: the self-trapping energy V_{st}, the nearest-neighbor shift V_{nn}, and the coincidence energy V_c. Right panels show the convergence of the classical migration barrier: V_m is the energy required to transfer the hydrogen over the saddle point via an adiabatic distortion of the host lattice. Lines are a guide to the eye only.

TABLE III. Vibrational states for hydrogen isotopes in Nb and Ta. The zero-point energy E_0 and the excitation energies $\hbar\omega_n$ are calculated in the self-trapped $1T$ configuration, whereas the corresponding bare tunneling matrix elements J_n are determined in the symmetric $2T$ configuration. All results in meV.

	Niobium		Tantalum	
	H	D	H	D
E_0	274	197	279	200
$\hbar\omega_1$	122	93	121	93
$\hbar\omega_2$	176	134	178	136
$\hbar\omega_3$	208	170	206	170
J_0	0.80	0.10	0.82	0.10
J_1	2.30	0.34	2.25	0.36
J_2	6.69[a]	1.42[a]	7.05[a]	1.52[a]
	0.15[a]	0.04[a]	0.15[a]	0.04[a]
J_3	16.1	7.77	17.1	8.32

[a]The second-excited state is twofold degenerated.

can be used to correct for the spurious forces arising due to the imposed periodicity. Still, the summation in Eq. (1) must be restricted in order to prevent the random noise of the vanishingly small forces acting on remote metal atoms from being weighted by the large distance. Therefore, when calculating P only metal atoms in the first two neighbor shells (corresponding to $d_1=\sqrt{5}a/4$ and $d_2=\sqrt{13}a/4$ for a T site and $d_1=a/2$ and $d_2=\sqrt{2}a/2$ for an O site) were included in the summation. The results, as given in Table II, agree well with those obtained by Elsässer *et al.*[13] using the same approximations. In particular, $\mathrm{Tr}P=11$ eV and only a small anisotropy for hydrogen at T sites in both Nb and Ta is in good agreement with experimental data from both Gorsky effect[25] and x-ray scattering[15,26] measurements. The calculated displacements of nearest-neighbor metal atoms upon relaxation are also given in Table II. The result $u_1=0.08$ Å for atoms surrounding an occupied T site is only slightly smaller than the experimental value 0.1 Å obtained from x-ray scattering.[27,28]

With hydrogen at the stable T site, we show the most important lattice energies for $\mathrm{Nb}_n\mathrm{H}$ and $\mathrm{Ta}_n\mathrm{H}$ as a function of hydrogen concentration $c=1/n$ in Fig. 1. Relaxation of metal atoms surrounding the impurity results in a stabilization of the system by the self-trapping energy $V_{\mathrm{st}}=189$ (185) meV for H-Nb (H-Ta) at low concentrations (cf. Table I). This configuration will be denoted by $1T$. If the hydrogen is moved to a nearest-neighbor T site in the distorted lattice, the energy increases by $V_{\mathrm{nn}}=80$ (78) meV. By instead relaxing the host lattice with the hydrogen extending over two neighboring T sites, a symmetric $2T$ configuration is obtained. We find a coincidence energy $V_c=V_{2T}-V_{1T}=19$ meV for hydrogen in both metals. Our calculated ratio V_c/V_{nn} is thus close to $1/4$ as expected from harmonic lattice theory.[1] For comparison we also show the classical migration barrier, which equals the extra energy required to bring the hydrogen to the relaxed saddle point S. We obtain $V_m=V_S-V_{1T}=148$ (180) meV for H-Nb (H-Ta) at low concentrations (cf. Table I).

B. Hydrogen vibrational states

For computational reasons, PES's for the hydrogen motion were mapped out using smaller supercells. By examining the convergence of the displacement fields of the self-trap and coincidence configuration, a hydrogen concentration of $1/16$ was found to be sufficiently small for reproducing most of the local relaxation effects (cf. also Fig. 1). At this concentration PES's for the hydrogen vibrational motion were mapped out. With the host lattice relaxed to $1T$ configuration the grid extend $a/2\times a/2\times a/2$ around the occupied site, and with the host lattice relaxed to the $2T$ configuration we used a twice as large grid rotated to enclose the coinciding sites. The grid spacing of first-principles data points was $a/8$ in both cases. Our calculated kinetic energies for the ground and lowest excited states of hydrogen isotopes in both metals can be found in Table III.

We start by considering hydrogen vibrating in the $1T$ configuration. In Fig. 2 the calculated wave functions for the ground and lowest vibrationally excited states of H are shown. The local symmetry of a relaxed T site is that of the D_{2d} point group. The ground state is therefore a fully symmetric A_1 state. For H we find excitation energies close to 120 meV for the first-excited B_2 state, 180 meV for the second-excited twofold-degenerated E state, and 210 meV for the third-excited A_1 state in both Nb and Ta. For D, these values are reduced by approximately a factor $0.9\times\sqrt{2}$. Our calculated excitation energies are only slightly larger than the values reported from inelastic neutron scattering experiments at low hydrogen concentrations.[29,30]

We next consider hydrogen in the $2T$ configuration. The change in zero-point energy compared to the self-trapped state was found to be small, only a few percent. The calculated ground-state tunneling matrix elements are $J_0=0.8(0.1)$ meV for H (D) in both Nb and Ta. Higher vibrational states have significantly larger overlaps. Tunneling matrix elements can, however, be expected to depend sensitively on the shape of the potential. For example, we have determined the PES's for a hydrogen concentration $c=1/16$. At lower concentrations the migration barriers were found to be reduced by nearly 20% in Nb and around 10% in Ta. This should increase the hop rate in the low-temperature regime. To investigate the sensitivity of the calculated tunneling matrix elements on the barrier height, we have scaled the PES's by a factor of 1.0 ± 0.2 and compared with the results thus

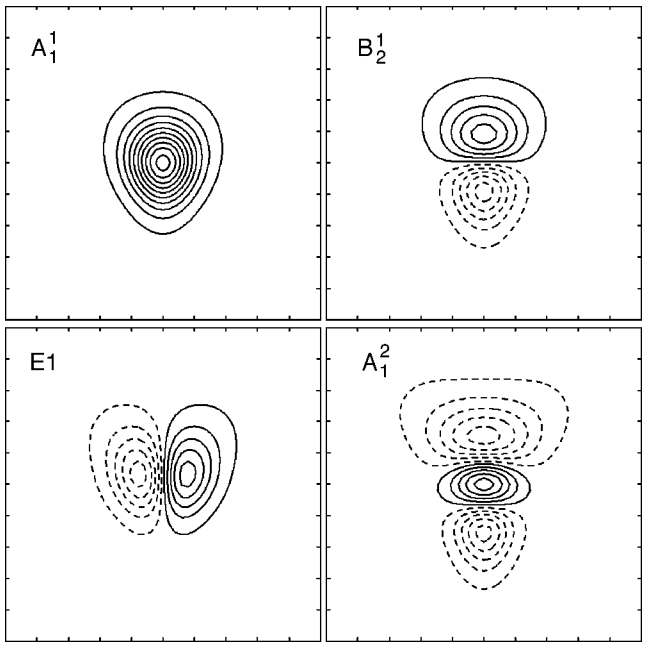

FIG. 2. Ground and vibrationally excited states for H self-trapped in the 1*T* configuration in Nb. Contours are drawn in a (001) plane through the stable site. Solid and dashed lines indicate different signs for the wave functions. The side length of each box is $a/2$, where $a=3.32$ Å is the lattice parameter.

obtained. With the modified potential we get the estimates $0.6<J_0<1.1$ meV ($0.06<J_0<0.2$ meV) for H (D) in both Nb and Ta.

C. Activation energies for diffusion

We finally consider hydrogen migration between the stable *T* sites in different temperature regimes. This is illustrated in Fig. 3. At low temperatures hydrogen diffusion is dominated by incoherent tunneling between ground states localized on neighboring interstitial sites. For multiphonon-assisted jumps Flynn and Stoneham[5] showed that the tunneling rate ν then is given by

$$\nu = \frac{\pi^{1/2}|J_0|^2}{2\hbar(E_c k_B T)^{1/2}} e^{-E_c/k_B T}, \tag{2}$$

where $E_c=E_{2T}-E_{1T}$ is the total energy required to create the ground-state coincidence configuration. The activation energy E_c is dominated by the potential part V_c, but there is also a kinetic contribution K_c that equals the change in zero-point energy (ZPE) between the 1*T* and 2*T* lattice configurations. These energies are given in the first part of Table IV.

Our calculated E_c is in very good agreement with NMR measurements of spin-lattice relaxation rates by Messer *et al.*[4] By fitting the parameters of Eq. (2) they obtain $E_c=27\pm2$ meV (32 ± 8 meV) and $J_0=0.9^{+0.1}_{-0.2}$ meV (0.7 ± 0.2 meV) for H-Nb (H-Ta). The agreement with the Gorsky effect measurements by Qi *et al.*[3] is not quite as good. It has, however, been argued that the NMR data are more reliable since they give information on the characteristic times for the elementary jump processes, while the measurements based on the Gorsky effect are more macroscopic in nature and may be affected by defects in the material.

At higher temperatures transitions between vibrationally excited states for the hydrogen motion start to contribute. This has been treated by Emin *et al.*[6] using the so-called occurrence probability approach. If the tunneling matrix elements are sufficiently large, an adiabatic picture becomes valid. The rate then takes the form $\nu=\nu_D \exp[-E_{\rm eff}/k_B T]$, where ν_D is the Debye frequency and the effective activation energy $E_{\rm eff}$ often is assumed to be given by the vibrational excitation energy $\hbar\omega_1$. A similar expression is obtained assuming the quantum-mechanically modified classical rate theory.[31] That approach predicts a rate $\nu=(k_B T/h)\exp[-\Delta F^{\ddagger}/k_B T]$, where $\Delta F^{\ddagger}$ is the free energy difference between the transition state and the stable site configurations. For motion of hydrogen in three dimensions, with the two

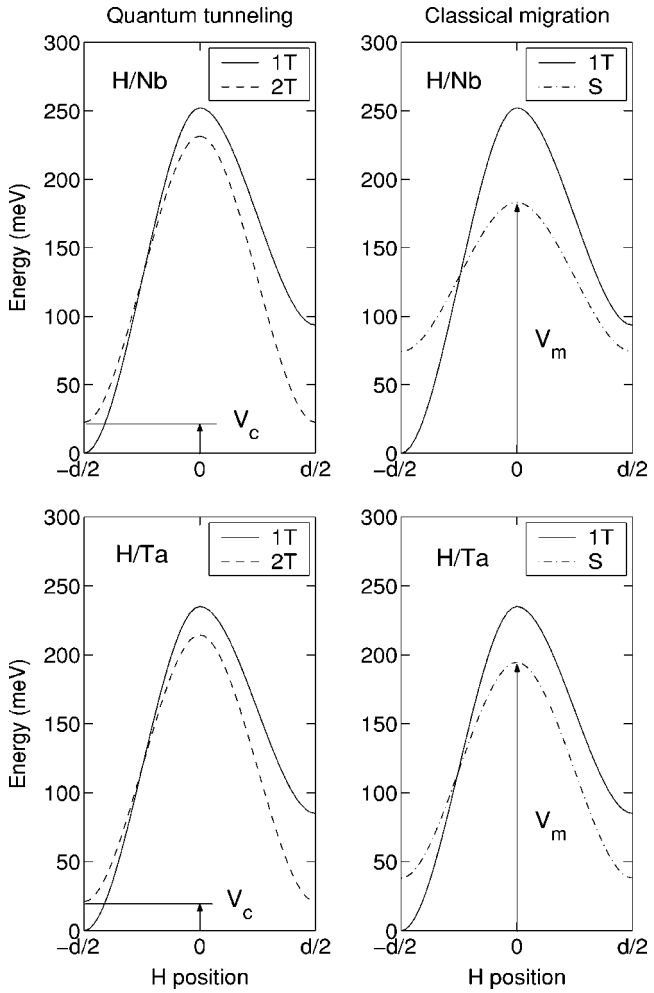

FIG. 3. Potential energy profiles when hydrogen is moved in a frozen host lattice configuration along a line connecting two adjacent *T* sites (separated by a distance $d=a/\sqrt{8}$), mapped out for a hydrogen concentration of 1/16 in Nb and Ta. The host lattice has been held fixed at the relaxed atomic positions corresponding to the self-trapped 1*T* (solid lines), the coincidence 2*T* (dashed lines) or the classical saddle-point *S* (dash-dotted lines) configurations. The activation energies for lattice-assisted quantum tunneling (V_c) and classical overbarrier migration (V_m) have been indicated in the figures.

TABLE IV. Hydrogen diffusion in the classical and quantum regimes. Activation energies for phonon assisted ground-state tunneling and classical overbarrier motion calculated for hydrogen migration between T sites. Potential energies are calculated for $c=1/54$, kinetic energies for $c=1/16$. All results in meV.

		Niobium		Tantalum	
		H	D	H	D
Quantum tunneling					
Potential	V_c	19.3		19.2	
Kinetic	K_c	+4.6	+3.8	+9.4	+7.1
Total	E_c	23.9	23.1	28.6	26.3
Classical migration					
Potential	V_m	147.8		179.7	
Kinetic	K_m	−21.6	−16.9	−14.6	−11.8
Total	E_m	126.2	130.9	165.1	167.9

bound degrees of freedom treated quantum mechanically ($k_BT \ll \hbar\omega_1$), one obtains $\nu=(k_BT/h)\exp[-E_m/k_BT]$.[35] Here $E_m=E_S-E_{1T}$ is the total energy required to bring the hydrogen from the self-trapped state to the classical saddle point. The activation energy E_m is dominated by the migration barrier V_m, but to fully account for the three-dimensional character of the problem, the ZPE for the perpendicular degrees of freedom along the reaction coordinate should also be included. This kinetic correction is estimated by solving for two-dimensional vibrational states at the dividing surface separating neighboring T sites in the coincidence configuration and subtracting the ground-state energy from the self-trapped configuration. The resulting effective barriers for H and D migration in Nb and Ta are summarized in the second part of Table IV.

Messer *et al.*[4] have also determined the the transition rate at higher temperatures $T>250$ K. They obtain an activation energy 119 meV (147 meV) and a prefactor 8.0×10^{12} s^{-1} (4.5×10^{12} s^{-1}) for the H-Nb (H-Ta) system. These experimental results can be interpreted in terms of either adiabatic tunneling transitions between excited states or classical over barrier motion, as the experimental activation energy is similar in magnitude to both the vibrational excitation energy $\hbar\omega_1$ (cf. Table III) and the classical migration energy E_m (cf. Table IV). However, the experimental trend with higher activation energy for H-Ta compared with H-Nb is only reproduced by the migration energy E_m. The experimental prefactor is consistent with both adiabatic transitions within the occurrence probability approach (the Debye frequency is $\nu_D=5.7\times10^{12}$ s^{-1} and $\nu_D=4.7\times10^{12}$ s^{-1} for Nb and Ta, respectively) and with the quantum-mechanically modified classical rate theory ($k_BT/h=6.3\times10^{12}$ s^{-1} at $T=300$ K).

IV. CONCLUSIONS AND OUTLOOKS

In conclusion, we have presented a first-principles density-functional study of hydrogen in Nb and Ta. The calculated energies, forces, and displacements for hydrogen self-trapped at tetrahedral sites in the lattice were all found to be in good agreement with experimental data. Motivated by their small mass, we have treated the motion of hydrogen atoms quantum mechanically. By mapping out three-dimensional PES's and solving a Schrödinger equation, ground and excited vibrational states for H and D were calculated for the $1T$ and $2T$ configurations. The resulting excitation energies are consistent with experiments. For hydrogen diffusion in the temperature range $100\text{ K}<T<200$ K the small-polaron theory of Flynn and Stoneham[5] was applied, and we found excellent agreement with NMR results for both the calculated coincidence energy and bare tunneling matrix elements. At higher temperatures our results indicate that hydrogen migration should best be described in terms of overbarrier motion, rather than tunneling from excited states.

It would be interesting to apply our approach to investigate diffusion in other H-metal systems. Recently, Wolverton *et al.*[32] published a systematic study of the structure and thermodynamics of H-Al. Another technologically relevant system is H-Fe, where an accurate description of hydrogen migration might result in a better understanding for the important problem of hydrogen embrittlement. The shorter lattice parameter of Fe (2.87 Å) compared to Nb and Ta in the present study (3.32 Å) suggests that tunneling phenomena might dominate the diffusion process at even higher temperatures.

ACKNOWLEDGMENTS

This work was supported by the Swedish Research Council (VR) and the Swedish Foundation for Strategic Research (SSF) via the ATOMICS program.

*Electronic address: sundell@fy.chalmers.se
†Electronic address: wahnstrom@fy.chalmers.se

[1] H. Grabert and H. R. Schober, in *Hydrogen in Metals III: Properties and Applications*, Vol. 73 of Topics in Applied Physics, edited by H. Wipf (Springer-Verlag, Berlin, 1997), Chap. 2.
[2] Y. Fukai, *The Metal-Hydrogen System* (Springer-Verlag, Berlin, 1993).
[3] Z. Qi, J. Völkl, R. Lässer, and H. Wenzl, J. Phys. F: Met. Phys. **13**, 2053 (1983).
[4] R. Messer, A. Blessing, S. Dais, D. Höpfel, G. Majer, C. Schmidt, A. Seeger, and W. Zag, Z. Phys. Chem., Neue Folge **2**, 61 (1986).
[5] C. P. Flynn and A. M. Stoneham, Phys. Rev. B **1**, 3966 (1970).
[6] D. Emin, M. I. Baskes, and W. D. Wilson, Phys. Rev. Lett. **42**, 791 (1979).
[7] H. Sugimoto and Y. Fukai, Phys. Rev. B **22**, 670 (1980).
[8] H. Sugimoto and Y. Fukai, J. Phys. Soc. Jpn. **50**, 3709 (1981).
[9] M. J. Puska and R. M. Nieminen, Phys. Rev. B **29**, 5382 (1984).
[10] A. Klamt and H. Teichler, Phys. Status Solidi B **134**, 103 (1986).
[11] A. Klamt and H. Teichler, Phys. Status Solidi B **134**, 533 (1986).
[12] C. Elsässer, K. M. Ho, C. T. Chan, and M. Fähnle, J. Phys.: Condens. Matter **4**, 5207 (1992).
[13] C. Elsässer, M. Fähnle, L. Schimmele, C. T. Chan, and K. M. Ho, Phys. Rev. B **50**, 5155 (1994).
[14] P. G. Sundell and G. Wahnström, Phys. Rev. Lett. **92**, 155901 (2004).
[15] H. Pfeiffer and H. Peisl, Phys. Lett. **60A**, 363 (1977).
[16] H. Krimmel, L. Schimmele, C. Elsässer, and M. Fähnle, J. Phys.: Condens. Matter **6**, 7679 (1994).
[17] G. Kresse and J. Hafner, Phys. Rev. B **48**, 13 115 (1993).
[18] G. Kresse and J. Furthmüller, Phys. Rev. B **54**, 11 169 (1996).
[19] P. E. Blöchl, Phys. Rev. B **50**, 17 953 (1994).
[20] Y. Wang and J. P. Perdew, Phys. Rev. B **44**, 13 298 (1991).
[21] H. J. Monkhorst and J. D. Pack, Phys. Rev. B **13**, 5188 (1976).
[22] M. Methfessel and A. T. Paxton, Phys. Rev. B **40**, 3616 (1989).
[23] H. Wenzl, Int. Met. Rev. **27**, 140 (1982).
[24] H. Kanzaki, J. Phys. Chem. Solids **2**, 21 (1957).
[25] G. Schaumann, J. Völkl, and G. Alefeld, Phys. Status Solidi **42**, 401 (1970).
[26] A. Magerl, B. Berre, and G. Alefeld, Phys. Status Solidi A **36**, 161 (1976).
[27] T. H. Metzger, H. Behr, G. Steyrer, and J. Peisl, Phys. Rev. Lett. **50**, 843 (1983).
[28] G. Steyrer, T. H. Metzger, and J. Peisl, J. Appl. Crystallogr. **17**, 33 (1984).
[29] R. Hempelmann, D. Richter, and A. Kollmar, Z. Phys. B: Condens. Matter **44**, 159 (1981).
[30] A. Magerl, J. J. Rush, and J. M. Rowe, Phys. Rev. B **33**, 2093 (1986).
[31] K. W. Kehr, in *Hydrogen in Metals I: Basic Properties*, Vol. 28 of Topics in Applied Physics, edited by G. Alefeld and J. Völkl (Springer-Verlag, Berlin, 1978), Chap. 8.
[32] C. Wolverton, V. Ozoliņš, and M. Asta, Phys. Rev. B **69**, 144109 (2004).
[33] The corresponding k-point mesh was $(12/N)\times(12/N)\times(12/N)$.
[34] We have used the LASO package, available from the Netlib repository (www.netlib.org).
[35] At high temperatures $k_BT>\hbar\omega_1$, where all degrees of freedom can be treated classically, this expression simplifies to $\nu=\nu_{\mathrm{H}}\exp[-V_m/k_BT]$.